

VOLUME 11
NUMBER 1
February
2009

FAR EAST JOURNAL OF DYNAMICAL SYSTEMS

- Alejandro Mesón and Fernando Vericat:** Estimates of large deviations in dynamical systems by a non-additive thermodynamic formalism 1
- V. Sundarapandian:** Necessary and sufficient conditions for local and global asymptotic stability of nonlinear cascade systems 17
- Shiro Ishikawa:** Ergodic problem in quantitative language 33
- Lasha Ephremidze and Nobuhiko Fujii:** The John-Nirenberg inequality for ergodic systems 49
- S. Khademloo and G. A. Afrouzi:** Existence of positive solutions of some quasilinear elliptic equation 57
- Yan-Long Li, Wu Min and Wei Zhang:** Influence of network topology on critical coupling parameter in synchronization of small world neural networks 65
- Yanxia Sun, Guoyuan Qi, Barend J. Van Wyk and Zenghui Wang:** Analysis of the Qi three dimensional chaotic system 77
- Ying Huang and Zhengde Dai:** Exact solitary wave solutions for a cubic 2D Ginzburg-Landau equation 95
- Huimei Wang and Zhiwei Xing:** Existence of positive periodic solution of an impulsive delay logistic model 107



PUSHPA PUBLISHING HOUSE

Vijaya Niwas, 198, Mumfordganj

Allahabad 211002, INDIA

e-mail: arun@pphmj.com

<http://www.pphmj.com>



ANALYSIS OF THE QI THREE DIMENSIONAL CHAOTIC SYSTEM

YANXIA SUN¹, GUOYUAN QI¹, BAREND J. VAN WYK¹ and
ZENGHUI WANG^{1,2}

¹F'SATLE

Tshwane University of Technology

Pretoria 0001, South Africa

²Department of Automation

Shandong University of Science and Technology

Qingdao 266510, P. R. China

Abstract

This paper applies the center manifold theorem to reduce the dimensions of the Qi three-dimensional system. Local bifurcation phenomena are analyzed, including the pitchfork and Hopf bifurcations of the chaotic system. The Poincaré map is also investigated. The analyses demonstrate the rich dynamics of the Qi chaotic system. Finally, the frequency spectral analysis shows that the system has a broad frequency bandwidth, which is desirable for engineering applications such as secure communications.

2000 Mathematics Subject Classification: 37D45.

Keywords and phrases: bifurcation, chaos, Hopf bifurcation, center manifold theorem, frequency spectral analysis.

This work was supported by grants from Innovative Research Foundation of Tshwane University of Technology, the National Scientific Foundation of China (10772135, 60774088) and the Scientific Foundation of Tianjin City, P. R. China (07JCYBJC05800), the Scientific and Technological Research Foundation of Ministry of Education, P. R. China (207005).

Received November 4, 2008

1. Introduction

With the advancement of chaos research, more and more chaos phenomena have been discovered in the mathematics, engineering and other fields. Many researchers have focused on the demonstration of chaos phenomena using simulation. The theoretical analyses of local and global characteristics and phenomena significantly have contributed to our understanding of the essence of chaos.

Qi et al. [7] proposed a three-dimensional nonlinear chaotic system which exhibited a rich dynamics. This system is quite different from previous systems such as the Lorenz [6], Alligood et al. [1], Rossler [10], Chen [3] and series Lorenz systems [5]. Every equation of the Qi system has a nonlinear term, making it more complex in dynamics than the former systems.

In this paper, two types of bifurcations are analyzed for the original Qi system, i.e., the pitchfork and Hopf bifurcations. The conditions of their existences are developed in detail by using the center manifold theorem and bifurcation theory. The Poincaré map and power spectrum exhibit the rich dynamic character of the Qi system [7].

2. Qi Three-dimensional Chaotic System and its Equilibrium Properties

The Qi system [7] is a three-dimensional continuous system described by

$$\begin{aligned}\dot{x} &= a(y - x) + yz, \\ \dot{y} &= cx - y - xz, \\ \dot{z} &= xy - bz,\end{aligned}\tag{1}$$

where a , b and c are all real constant parameters. This system has five equilibria. Note that system (1) is invariant under the coordinate transformation $(x, y, z) \rightarrow (-x, -y, z)$, i.e., the system is symmetrical about z -axis.

Figure 1 shows the spectrum of Lyapunov exponents of system (1)

with respect to parameter c . The largest Lyapunov exponent can reach a value of 10, which is big different from those of the Lorenz system and the Chen system with 0.9 and 2, respectively. As can be seen from Figure 1, the nonlinear system displays chaos, and the positive Lyapunov exponents are high in a large range of parameters.

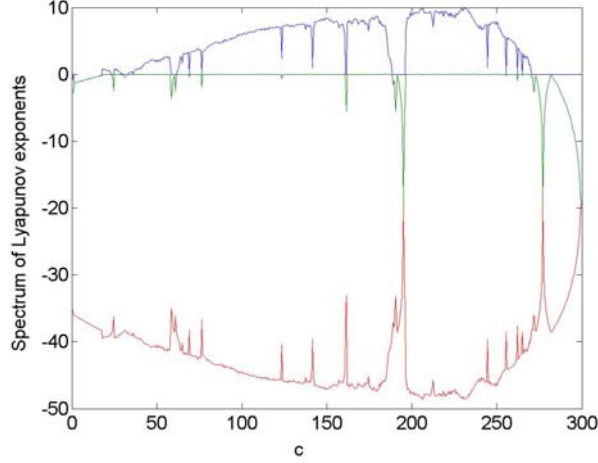


Figure 1. Spectrum of Lyapunov exponents of system (1) with $a = 35$, $b = 8/3$.

Let

$$d = -2ab + abc + bc^2, \quad e = \sqrt{b^2c^2(-4a + a^2 + 2ac + c^2)}, \quad f = abc + bc^2, \quad (2)$$

$$x^1 = \frac{\sqrt{2}}{2} \sqrt{\frac{d+e}{a}}, \quad x^2 = \frac{\sqrt{2}}{2} \sqrt{\frac{d-e}{a}},$$

$$y^1 = \sqrt{2}bc\sqrt{\frac{d+e}{a}} \frac{a}{f+e}, \quad y^2 = \sqrt{2}bc\sqrt{\frac{d-e}{a}} \frac{a}{f-e},$$

$$z^1 = \frac{(d+e)c}{f+e}, \quad z^2 = \frac{(d-e)c}{f-e}, \quad (3)$$

the following five equilibria are found:

$$S_1 = [0, 0, 0], \quad S_2 = (x^1, y^1, z^1), \quad S_3 = (-x^1, -y^1, z^1),$$

$$S_4 = (x^2, y^2, z^2), \quad S_5 = (-x^2, -y^2, z^2). \quad (4)$$

It can easily be verified that when $d - e < 0$, x^2, y^2 are complex. So only S_1, S_2 and S_3 are the equilibria of the system. By linearizing system (1) at S_1 , one obtains the Jacobian

$$\begin{bmatrix} -a & a & 0 \\ c & -1 & 0 \\ 0 & 0 & -b \end{bmatrix}. \quad (5)$$

And its characteristic equation,

$$f(\lambda) = (\lambda + b)(\lambda^2 + (a + 1)\lambda + a - ac) = 0. \quad (6)$$

It is obvious that $-b$ is one of the roots of (6), and the other two roots do not always have negative real parts according to the Routh-Hurwitz condition.

3. Bifurcations of Origin

3.1. Pitchfork bifurcation of S_1

From (6) with $c = 1$, we have $\lambda_1 = 0, \lambda_2 = -(a + 1) < 0, \lambda_3 = -b < 0$, and the corresponding eigenvectors are

$$v_1 = [1, 1, 0]^T, \quad v_2 = [a, -1, 0]^T, \quad v_3 = [0, 0, 1]^T. \quad (7)$$

According to the center manifold theorem [12], the topological structure of system (1) will change and generate pitchfork bifurcation because of $\lambda_1 = 0$, where c is the local bifurcation parameter at 1.

Within the neighborhood of $c = 1$, let $c = 1 + \xi$ with ξ sufficiently small. Then we have

$$\begin{aligned} \lambda_1 &= -\frac{a+1}{2} + \frac{1}{2}\sqrt{(a+1)^2 + 4a(c-1)} \\ &= \frac{a+1}{2} \left(-1 + \sqrt{1 + \frac{4a\xi}{(a+1)^2}} \right) \\ &= \frac{a+1}{2} \left(-1 + \left(1 + \frac{2a\xi}{(a+1)^2} + o(\xi^2) \right) \right) \\ &= \frac{a\xi}{(a+1)} + o(\xi^2), \end{aligned} \quad (8)$$

where Taylor expansion is used. By utilizing the eigenvectors to construct a new vector space, we obtain the following transformation:

$$\begin{bmatrix} x \\ y \\ z \end{bmatrix} = \begin{bmatrix} 1 & a & 0 \\ 1 & -1 & 0 \\ 0 & 0 & 1 \end{bmatrix} \begin{bmatrix} u \\ v \\ w \end{bmatrix}. \quad (9)$$

Thus the system is transformed into the form

$$\begin{bmatrix} \dot{u} \\ \dot{v} \\ \dot{w} \end{bmatrix} = \begin{bmatrix} 0 & 0 & 0 \\ 0 & -(a+1) & 0 \\ 0 & 0 & -b \end{bmatrix} \begin{bmatrix} u \\ v \\ w \end{bmatrix} + \begin{bmatrix} g_1 \\ g_2 \\ g_3 \end{bmatrix}, \quad (10)$$

where

$$g_1 = \frac{((1-a)uv - (a^2+1)uw)}{a+1},$$

$$g_2 = \frac{(2uw + (a-1)vw)}{a+1},$$

$$g_3 = u^2 - av^2 + (a-1)uv.$$

Since $\lambda_1 = 0$, $\lambda_2, \lambda_3 < 0$, there exists a center manifold which is tangent to the u axis. The center manifold is expressed as

$$W^c(S_1) = \{(u \ v \ w) \in R^3 \mid v = h_1(u), w = h_2(u), |u| < \delta, \\ h_i(0) = 0, Dh_i(0) = 0, i = 1, 2\}. \quad (11)$$

Here δ is sufficiently small. To seek the center manifold $W^c(S_1)$, we assume that $h_1(u)$ and $h_2(u)$ have the forms:

$$v = h_1(u) = a_1u^2 + b_1u^3 + c_1u^4 + \dots,$$

$$w = h_2(u) = a_2u^2 + b_2u^3 + c_2u^4 + \dots. \quad (12)$$

Substituting (12) into the second and third equations of (10), respectively, and comparing the coefficients of u^2, u^3, u^4 , we have two sets of

equations. The first set of equations is

$$\begin{cases} 0 = -(a+1)a_1, \\ 0 = \frac{2a_2}{a+1} - (a+1)b_1, \\ \frac{1}{a+1}(2a_1a_2(1-a)) = -(a+1)c_1 + \frac{2b_2}{a+1} + \frac{(a-1)a_1a_2}{a+1}. \end{cases} \quad (13)$$

The second set of equations is

$$\begin{cases} 1 - ba_2 = 0, \\ (a-1)a_1 - bb_2 = 0, \\ \frac{2(1-a)a_2^2}{a+1} = (a-1)b_1 - bc_2 - aa_1^2. \end{cases} \quad (14)$$

Solving equations (13) and (14) simultaneously, we have

$$\begin{aligned} a_1 = 0, \quad b_1 &= \frac{2}{(a+1)^2b}, \quad c_1 = 0, \\ a_2 &= \frac{1}{b}, \quad b_2 = 0, \quad c_2 = \frac{2(a^2 + ab - b - 1)}{(a+1)^2b^3}. \end{aligned} \quad (15)$$

Thus the following center manifold equations are obtained:

$$\begin{aligned} v &= h_1(u) = \frac{2}{(a+1)^2b} u^3 + o(u^5), \\ w &= h_2(u) = \frac{1}{b} u^2 + \frac{2(a^2 + ab - b - 1)}{(a+1)^2b^3} u^4 + o(u^5). \end{aligned} \quad (16)$$

Finally, substituting (16) into (10), a one-dimensional (1-D) reduced vector field,

$$\begin{aligned} \dot{u} &= \lambda_1 u + \frac{1-a}{(a+1)b} u^3 + o(u^5) = \frac{a\xi}{(a+1)} u + \frac{1-a}{(a+1)b} u^3 + o(u^5), \\ \dot{\xi} &= 0 \end{aligned} \quad (17)$$

is obtained based on the center manifold theory, which can be used to investigate the bifurcation. We now can compute the center manifold with

an accuracy of order 3, which is sufficient to answer questions of stability.

Let $\dot{u} = f(u, \xi) = 0$, and ignoring the term $o(u^5)$ in (17), we have

$$f(0, 0) = 0, \quad \left. \frac{\partial f}{\partial u} \right|_{(0,0)}, \quad \left. \frac{\partial f}{\partial \xi} \right|_{(0,0)} = 0,$$

$$\left. \frac{\partial^2 f}{\partial u^2} \right|_{(0,0)} = 0, \quad \left. \frac{\partial^2 f}{\partial u \partial \xi} \right|_{(0,0)} = \frac{a}{a+1} \neq 0, \quad \left. \frac{\partial^3 f}{\partial u^3} \right|_{(0,0)} = \frac{6(1-a)}{(a+1)b} \neq 0.$$

According to the theorem [12], the equilibrium point $(u, \xi) = (0, 0)$ undergoes a pitchfork bifurcation at $u = 0$. Furthermore, let

$$\frac{a\xi}{(a+1)}u + \frac{1-a}{(a+1)b}u^3 = 0, \tag{18}$$

we have $u_1 = 0$, $u_{2,3} = \pm \sqrt{\frac{ab\xi}{(a-1)}}$, ($a > 1$).

Hence, about the equilibria of (18), under the condition $a > 1$ we have

(1) when $-1 < \xi < 0$, i.e., $0 < c < 1$, the reduced 1-D system (18) has only one equilibrium at origin $u_1 = 0$ because $u_{2,3}$ are a pair of imaginary numbers;

(2) when $\xi > 0$, i.e., $c > 1$ it has three equilibria at $u_1 = 0$, $u_{2,3} = \pm \sqrt{\frac{ab\xi}{(a-1)}}$, ($a > 1$), respectively.

Furthermore, we have

$$\left. \frac{\partial f(\xi, u)}{\partial u} \right|_{u=u_1} = \frac{a\xi}{a+1} \begin{cases} > 0, \xi > 0, \\ < 0, \xi < 0, \end{cases} \tag{19}$$

$$\left. \frac{\partial f(\xi, u)}{\partial u} \right|_{u=u_{2,3}} = \frac{-2a\xi}{a+1} < 0, \xi > 0. \tag{20}$$

Therefore, when $-1 < \xi < 0$, the only one equilibrium u_1 of system (18) is a sink. At $\xi = 0$, i.e., $c = 1$, system (18) undergoes pitchfork bifurcation from one equilibrium into three equilibria. When $\xi > 0$, the equilibrium

u_1 becomes a source, and another two equilibria $u_{2,3}$ come out and are sinks. From (18), with the parameter changing of the system, the range of ξ accordingly changes.

The diagram of the pitchfork bifurcation of equation (18) is shown in Figure 2. The blue lines denote the trajectories of stable equilibrium with parameter ξ increasing, and the red line denotes the trajectory of the unstable equilibrium. It is notable that in the neighborhood of S_1 , $\xi = 0$ corresponds to the bifurcation parameter $c = 1$. Therefore, system (1) undergoes a pitchfork bifurcation at $c = 1$. Correspondingly, the system has only one globally stable equilibrium when $-1 < \xi < 0$. It has three equilibria in which the origin is stable, while another two non-zero equilibria are unstable when $\xi > 0$. The diagram of pitchfork bifurcation of system (1) with parameter changing is shown in Figure 3 where the curves with arrows show that although the two orbits of system (1) start from the neighborhood of the origin (a saddle) are attracted into the non-zero equilibria, respectively.

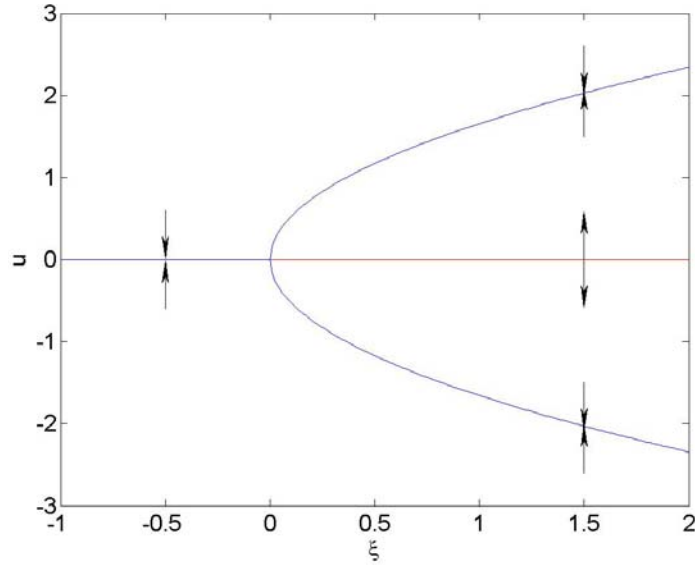


Figure 2. The diagram of the pitchfork bifurcation based on system (18).

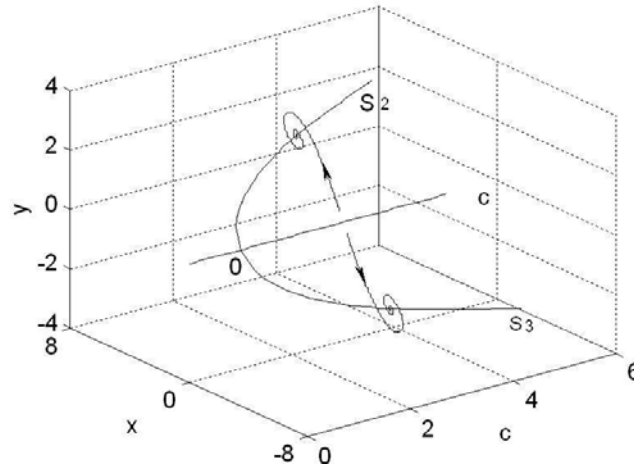


Figure 3. The diagram of the pitchfork bifurcation based on system (1).

We therefore obtain the following theorem:

Theorem 1. *Under condition $a > 1$ and ξ sufficiently small, on the line $c = 1$, system (1) undergoes a pitchfork bifurcation at origin $S_1 = [0 \ 0 \ 0]$. For $c = 1 + \xi$ and $-1 < \xi < 0$, there is one equilibrium $S_1 = [0 \ 0 \ 0]$, and S_1 is a sink. For $c = 1 + \xi$ and $\xi > 0$, two new equilibria $S_2 = (x^1, y^1, z^1)$ and $S_3 = (-x^1, -y^1, z^1)$ emerge and are sinks while S_1 becomes a source.*

3.2. Hopf bifurcation of S_1

In this section, we deal with another kind of bifurcation at origin $S_1 = [0 \ 0 \ 0]$ of system (1) using an analytical method. From (6), we have these three eigenvalues at origin.

$$\lambda_{1,2} = (-a - 1 \pm \sqrt{a^2 - 2a + 4ac + 1})/2 = \sigma(a) \pm iw \text{ and } \lambda_3 = -b. \quad (21)$$

The existence of Hopf bifurcation of equilibrium has three following conditions [12]:

- (1) The eigenvalues cross the imaginary axis transversely.
- (2) The coefficient Λ_1 in the Poincaré-Andronov-Hopf normal form is nonzero.

It is easy to get

$$\rho_1 = \frac{d\sigma(a)}{da} = -\frac{1}{2}, \quad (22)$$

so the first condition of the Hopf bifurcation is satisfied. Now we investigate the second condition. Suppose the characteristic equation (6) has pure imaginary roots $\lambda_{1,2} = \pm iw$ ($w > 0$). When $a = a_0 = -1$ the Jacobian matrix of system (1) has a pair of imaginary eigenvalues and one negative real eigenvalue, i.e.,

$$\lambda_{1,2} = \pm iw_0, \quad w(a_0) = w_0 = \sqrt{c-1}, \quad c > 1, \quad \lambda_3 = -b \quad (23)$$

and the corresponding eigenvectors

$$v_1 = \begin{bmatrix} \frac{wi}{c} & 1 & 0 \end{bmatrix}^T, \quad v_2 = \begin{bmatrix} \frac{-wi}{c} & 1 & 0 \end{bmatrix}^T, \quad v_3 = [0 \quad 0 \quad 1]^T. \quad (24)$$

By utilizing the real generalized eigenvectors as the basis of new coordinates, we obtain the transformation

$$\begin{pmatrix} x \\ y \\ z \end{pmatrix} = \begin{bmatrix} \omega & -\omega^2 & 0 \\ \omega & 0 & 0 \\ 0 & 0 & 1 \end{bmatrix} \begin{pmatrix} x_1 \\ y_1 \\ z_1 \end{pmatrix}. \quad (25)$$

System (1) becomes

$$\begin{pmatrix} \dot{x}_1 \\ \dot{y}_1 \\ \dot{z}_1 \end{pmatrix} = \begin{bmatrix} 0 & -\omega & 0 \\ \omega & 0 & 0 \\ 0 & 0 & -b \end{bmatrix} \begin{pmatrix} x_1 \\ y_1 \\ z_1 \end{pmatrix} + \begin{pmatrix} f^1 \\ f^2 \\ f^3 \end{pmatrix}. \quad (26)$$

Here

$$f^1 = \frac{1}{c}(\omega y_1 - x_1)z_1,$$

$$f^2 = -\frac{1}{\omega}x_1z_1 + \frac{1}{c\omega}(\omega y_1 - x_1)z_1,$$

$$f^3 = \omega^2x_1^2 - \omega^3x_1y_1.$$

Thus according to the center manifold theorem, there exists a center manifold for (26), which could be represented locally by

$$\begin{aligned} W^c(S_1) &= \{(x_1 \quad y_1 \quad z_1) \in R^3 \mid z_1 \\ &= h(x_1, y_1), \mid x_1, y_1 \mid < \delta, h(0, 0) = 0, Dh(0, 0) = 0\}, \end{aligned} \quad (27)$$

where δ is sufficiently small. We assume that

$$\begin{aligned} z_1 &= h(x_1, y_1) \\ &= d_1 x_1^2 + d_2 x_1 y_1 + d_3 y_1^2 + d_4 x_1^3 + d_5 x_1^2 y_1 + d_6 x_1 y_1^2 + d_7 y_1^3 \dots \end{aligned} \quad (28)$$

The center manifold can be approximately computed by substituting (28) into (26) and comparing the coefficients, to obtain

$$\begin{aligned} d_1 &= \frac{b\omega^2 + \omega^3}{b^2 + 2\omega^2}, \quad d_2 = \frac{2\omega^3 - b\omega^2}{b^2 + 2\omega^2}, \quad d_3 = \frac{2\omega^3 - b\omega^2}{b(b^2 + 2\omega^2)}, \\ d_4 &= 0, \quad d_5 = 0, \quad d_6 = 0, \quad d_7 = 0. \end{aligned} \quad (29)$$

The vector field reduced to the center manifold is therefore given by

$$\begin{bmatrix} \dot{x}_1 \\ \dot{y}_1 \end{bmatrix} = \begin{bmatrix} 0 & -\omega_0 \\ \omega_0 & 0 \end{bmatrix} \begin{bmatrix} x_1 \\ y_1 \end{bmatrix} + \begin{bmatrix} f_1(x_1, y_1) \\ f_2(x_1, y_1) \end{bmatrix}, \quad (30)$$

where

$$\begin{aligned} f_1(x_1, y_1) &= f_1(x_1, y_1, h(x_1, y_1)), \\ f_2(x_1, y_1) &= f_2(x_1, y_1, h(x_1, y_1)). \end{aligned} \quad (31)$$

The index number Λ_1 can be computed as

$$\begin{aligned} \Lambda_1 &= \frac{1}{16} [f_{x_1 x_1 x_1}^1 + f_{x_1 y_1 y_1}^1 + f_{x_1 x_1 y_1}^2 + f_{y_1 y_1 y_1}^2] \\ &+ \frac{1}{16\omega_0} [f_{x_1 y_1}^1 (f_{x_1 x_1}^1 + f_{y_1 y_1}^1) - f_{x_1 y_1}^2 (f_{x_1 x_1}^2 + f_{y_1 y_1}^2) \\ &\quad - f_{x_1 x_1}^1 f_{x_1 x_1}^2 + f_{y_1 y_1}^1 f_{y_1 y_1}^2] \\ &= \frac{1}{16} \left(\frac{2d_1}{c} + \left(\frac{2\omega}{c} - \frac{2}{\omega} - \frac{2}{c\omega} \right) d_2 - \frac{2d_3}{c} \right). \end{aligned} \quad (32)$$

To meet the condition of index number $\Lambda_1 \neq 0$, we have

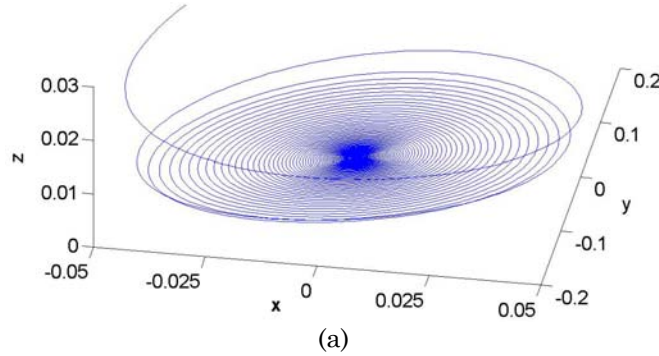
$$\frac{2d_1}{c} + \left(\frac{2\omega}{c} - \frac{2}{\omega} - \frac{2}{c\omega} \right) d_2 - \frac{2d_3}{c} \neq 0. \quad (33)$$

Therefore, the second condition of Hopf bifurcation is met. From (22) and (33), we have the conditions of Hopf bifurcation as follows:

$$c > 1, \quad \frac{2d_1}{c} + \left(\frac{2\omega}{c} - \frac{2}{\omega} - \frac{2}{c\omega} \right) d_2 - \frac{2d_3}{c} \neq 0. \quad (34)$$

Theorem 2. *If the parameters of system (1) meet condition (34), system (1) undergoes a Poincaré-Andronov-Hopf bifurcation (Hopf bifurcation) at origin $S_1 = [0 \ 0 \ 0]$. A transition from sink to periodic motion occurs. Moreover, since $\rho_1 = -\frac{1}{2} < 0$, the periodic solution emerging after $a > -1$, is stable if $\Lambda_1 < 0$, and is unstable if $\Lambda_1 > 0$.*

For example, when $a = b = 1$, $c = 10$, we have $\Lambda_1 = -0.0257$, $\rho_1 = \frac{d\alpha(a)}{da} \Big|_{a=1} = -\frac{1}{2} < 0$. According to Theorem 2, the stable periodic orbits emerge from zero equilibrium when $a < -1$. Select $[0.05, 0.05, 0.05]$ as the initial states in the neighborhood of the origin. When $a > -1$ the zero equilibrium is stable, and thus the system orbit is attracted to zero as shown in Figure 4(a), when $a < -1$, the system orbit is attracted to a stable periodic orbit, at the same time, the zero equilibrium becomes unstable as shown in Figure 4(b). When $a < -1$ the limit circle is shown clearly in Figure 5.



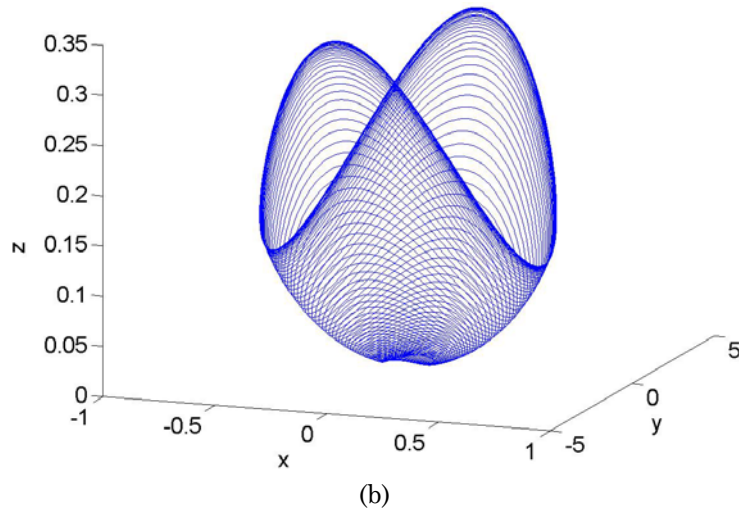


Figure 4. Hopf bifurcation in system (1) according to Theorem 2. (a) $a = -0.95 > -1$, (b) $a = -1.05 < -1$.

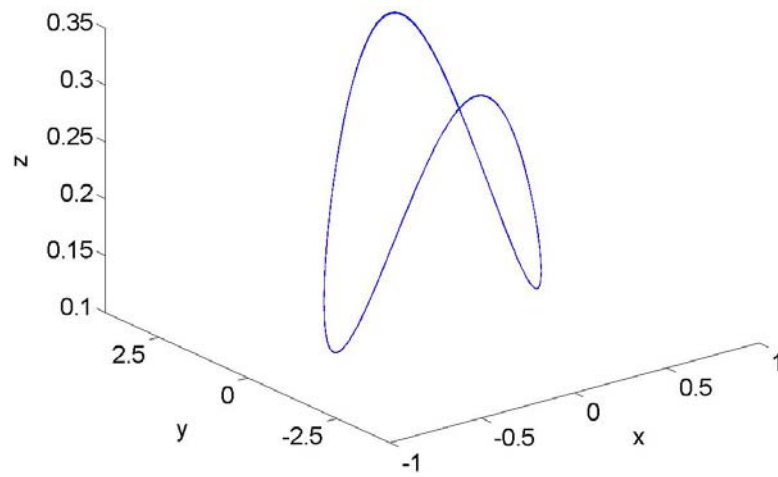
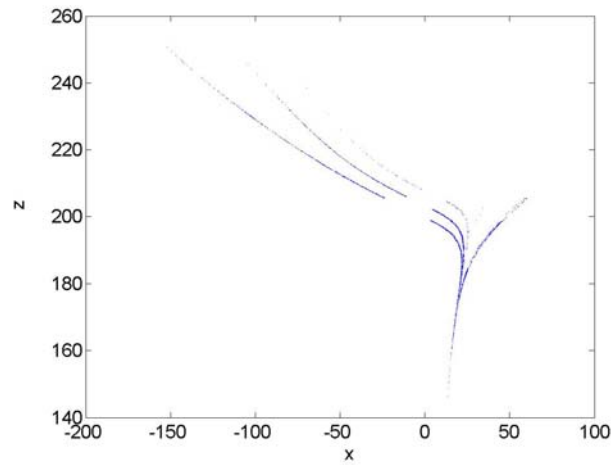


Figure 5. The limit circle omitting the transient response when $a = -1.05 < -1$.

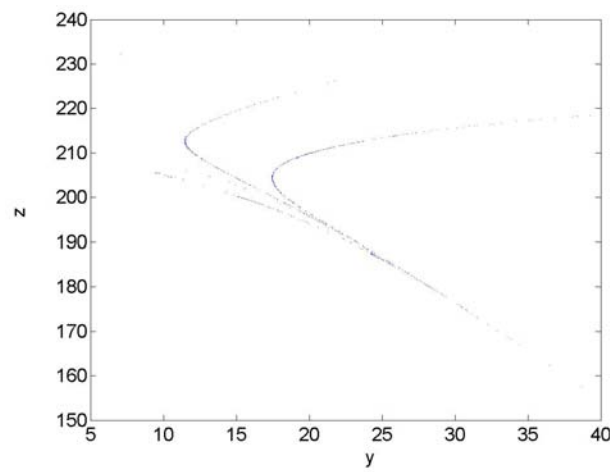
4. Poincaré Map of the Chaotic Attractor

As an important analysis technique, the Poincaré map can reveal bifurcation and folding properties of chaos. When $a = 35$, $b = 8/3$,

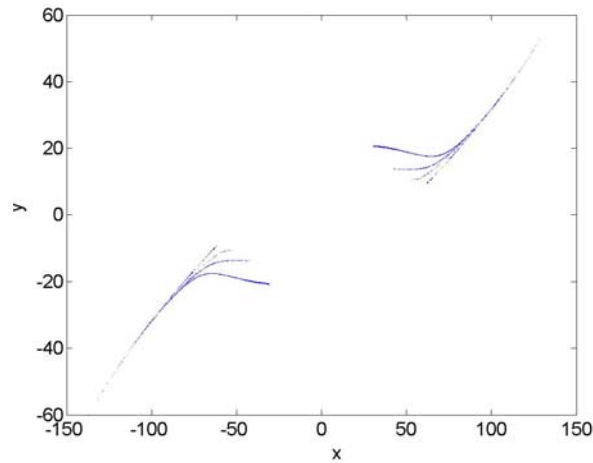
$c = 206$, one may take the equilibrium value of S_2 , i.e., $x = x^1$, $y = y^1$, and $z = z^1$ as crossing planes, respectively, where $x^1 = 61.4622$, $y^1 = 8.9314$, and $z^1 = 205.8547$. Figures 6(a-c) show the Poincaré maps on different crossing planes. They indicate that the system has extremely rich dynamics.



(a) Poincaré map on the crossing section $x = x^1$.



(b) Poincaré map on the crossing section $y = y^1$.



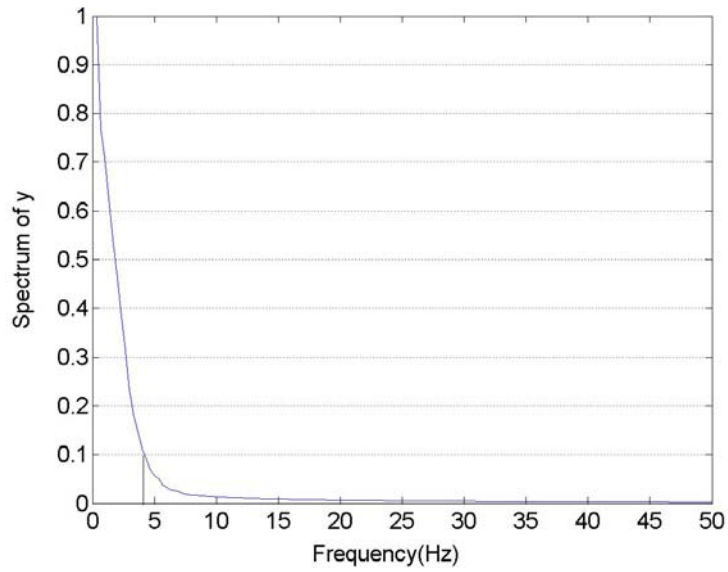
(c) Poincaré map on the crossing section $z = z^1$.

Figure 6. Poincaré maps on different crossing sections when $a = 35$, $b = 8/3$, $c = 206$.

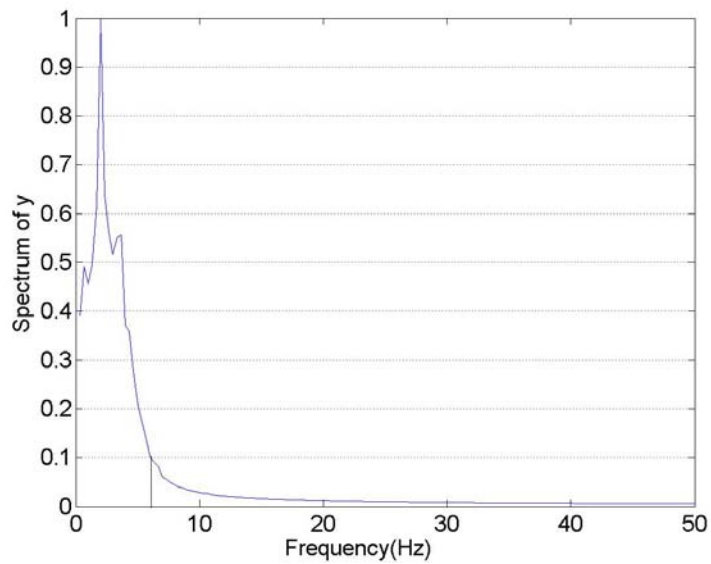
5. Frequency Spectral Analysis

Many proposed chaos-based encryption schemes have been totally or partially broken by different attacks [8, 9, 11]. One of the reasons is that the degree of randomness and disorder of simple chaotic signals are not high enough as reflected by their narrow bandwidths. Recall that the bandwidths of the Lorenz and Chen systems are approximately between 0 and 5.8Hz and therefore cannot be used to completely mask the messages in real communication applications. Once intercepted, there is a high possibility that the messages can be extracted. Figures 7(a) and (b) show the frequency spectra of the Lorenz and Chen systems, respectively.

However, the frequency spectrum of the Qi system has very wide bandwidth as shown in Figure 8. The bandwidth of signal y is about 35Hz, which is nearly 10 times wider than that of the Lorenz system, which could be advantageous to secure communication applications.

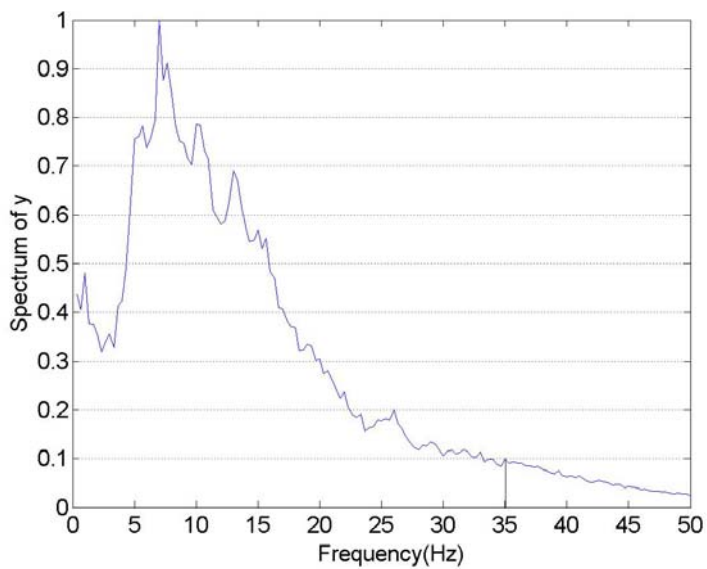


(a) The Lorenz system with $a = 10$, $b = 8/3$, $c = 28$.

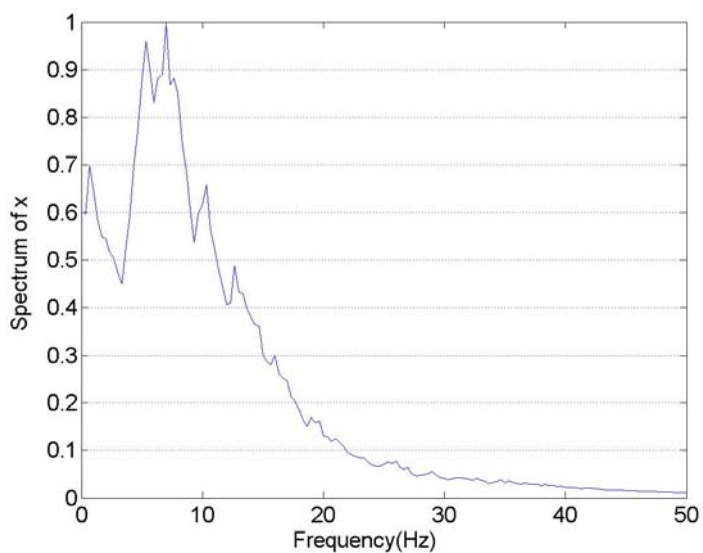


(b) The Chen system with $a = 35$, $b = 8/3$, $c = 28$.

Figure 7. The frequency spectra generated numerically from several typical chaotic systems.



(a) spectrum of y .



(b) spectrum of x .

Figure 8. The frequency spectra generated numerically from Qi chaotic systems with $a = 35$, $b = 8/3$, $c = 206$.

6. Conclusion

In this paper, the pitchfork and Hopf bifurcations, the poincaré map and frequency spectrums of the Qi three dimensional chaos system have been investigated. Based on a rigorous theoretical analysis, the stability of the fixed points when the bifurcation parameter passes the pitchfork bifurcation point has been analyzed. The bifurcation of the period cycle emerging from the zero equilibrium as can be seen from the Hopf bifurcation analysis was also investigated. The frequency spectral analysis shows that the system has a very wide frequency bandwidth, which is very desirable for engineering applications such as secure communications.

References

- [1] K. Alligood, T. Sauer and J. Yorke, *Chaos: An Introduction to Dynamical Systems*, 3rd ed., Springer-Verlag, New York, 2000.
- [2] G. Chen and J. Lü, *Dynamic Analysis, Control and Synchronization for Lorenz System Family*, Science Press, Beijing, 2003.
- [3] G. Chen and T. Ueta, Yet another chaotic attractor, *Int. J. Bifur. Chaos* 9 (1999), 1465-1466.
- [4] M. W. Hirsch and S. Smale, *Differential Equations, Dynamical Systems, and Linear Algebra*, Academic Press, New York, Heidelberg, Berlin, 1974.
- [5] T. Li, G. Chen and Y. Tang, On stability and bifurcation of Chen's system, *Chaos Solutions Fractals* 19 (2004), 1269-1282.
- [6] J. Lu, D. Cheng and S. Celikovsky, Bridge the gap between the Lorenz system and the Chen system, *Int. J. Bifur. Chaos* 12 (2002), 2917-2926.
- [7] G. Qi, G. Chen and S. Du, Analysis of a new chaotic system, *Physic A* 352 (2005), 295-308.
- [8] G. Qi, M. A. van Wyk and B. J. van Wyk, On a new hyperchaotic system, *Phys. Lett. A* 372 (2007), 124-136.
- [9] G. Qi, G. Chen, M. A. van Wyk, B. J. van Wyk and Y. Zhang, Four-wing chaotic attractor generated from a new 3-D quadratic chaotic system, *Chaos Solitons Fractals*, 2007 (in press and available online).
- [10] O. Rossler, An equation for hyperchaos, *Phys. Lett. A* 71 (1979), 155-157.
- [11] T. Ueta and G. Chen, Bifurcation analysis of Chen's attractor, *Int. J. Bifur. Chaos* 10 (2000), 917-931.
- [12] S. Wiggins, *Introduction to Applied Nonlinear Dynamical Systems and Chaos*, Springer-Verlag, New York, 2003.